Specific and flexible roles of heparan sulfate modifications in *Drosophila* FGF signaling

Keisuke Kamimura,[1,2] Takashi Koyama,[1] Hiroko Habuchi,[2] Ryu Ueda,[3] Masayuki Masu,[4] Koji Kimata,[2] and Hiroshi Nakato[1]

[1]Department of Genetics, Cell Biology, and Development, The University of Minnesota, Minneapolis, MN 55455
[2]Institute for Molecular Science of Medicine, Aichi Medical University, Aichi 480-1195, Japan
[3]Invertebrate Genetics Laboratory, Genetic Strain Research Center, National Institute of Genetics, Mishima, Shizuoka 411-8540, Japan
[4]Department of Molecular Neurobiology, Institute of Basic Medical Sciences, Graduate School of Comprehensive Human Sciences, University of Tsukuba, Ibaraki 305-8577, Japan

Specific sulfation sequence of heparan sulfate (HS) contributes to the selective interaction between HS and various proteins in vitro. To clarify the in vivo importance of HS fine structures, we characterized the functions of the *Drosophila HS 2-O* and *6-O sulfotransferase* (*Hs2st* and *Hs6st*) genes in FGF-mediated tracheal formation. We found that mutations in *Hs2st* or *Hs6st* had unexpectedly little effect on tracheal morphogenesis. Structural analysis of mutant HS revealed not only a loss of corresponding sulfation, but also a compensatory increase of sulfation at other positions, which maintains the level of HS total charge. The restricted phenotypes of *Hsst* mutants are ascribed to this compensation because FGF signaling is strongly disrupted by *Hs2st; Hs6st* double mutation, or by overexpression of 6-*O* sulfatase, an extracellular enzyme which removes 6-*O* sulfate groups without increasing 2-*O* sulfation. These findings suggest that the overall sulfation level is more important than strictly defined HS fine structures for FGF signaling in some developmental contexts.

Introduction

Secreted signaling proteins, such as BMPs, Wnts, Hedgehog, and FGFs, play key roles in animal development. Although it is established that reception of these molecules on the cell surface is mediated by heparan sulfate proteoglycans (HSPGs), the mechanism producing selective binding of proteins to heparan sulfate (HS) in a growth factor–rich environment remains a fundamental question. HS is synthesized as disaccharide polymers, which then undergoes a series of modification events including *N*, 2-*O*, 6-*O*, and 3-*O* sulfation. A number of in vitro studies showed that interactions between HS and various growth factors require unique HS structures in which 2-*O* and 6-*O* sulfate groups contribute to generate specific sulfation patterns (for reviews see Nakato and Kimata, 2002; Habuchi et al., 2004). Crystallographic studies also supported this biochemical evidence, showing that the 2-*O* and 6-*O* sulfate groups form hydrogen bonds with heparin binding residues of FGFs and/or FGF receptors (FGFRs) to induce dimerization of FGFRs (Schlessinger et al., 2000). Thus, in vitro studies showed that specific sulfation patterns on HS have critical roles in its selective binding to ligand proteins. However, the in vivo importance of these sulfation events is poorly understood.

FGF signaling regulates tracheal system formation in *Drosophila* (Klambt et al., 1992; Sutherland et al., 1996). The tracheal precursor cells express Breathless (Btl), a *Drosophila* FGF receptor, and migrate toward regions expressing Branchless (Bnl; a *Drosophila* FGF) to form primary branches in the embryo. FGF also controls the formation of the adult tracheal system, the air sac, which develops from a group of cells called "tracheoblasts" in the wing disc (Sato and Kornberg, 2002). A previous study showed that Btl-dependent activation of MAP kinase relies on *sulfateless* (*sfl*), which encodes *N*-deacetylase/*N*-sulfotransferase (NDST), indicating that HS has a crucial role in these processes (Lin et al., 1999). Because the reaction catalyzed by NDST is the first step in HS modification and is critical for subsequent reactions, mutation of *sfl* results in the production of sugar chains with no sulfation (Toyoda et al., 2000). To determine what structural features of HS are required for regulating FGF signaling, we characterized functions of *HS 2-O sulfotransferase* (*Hs2st*) and *HS 6-O sulfotransferase* (*Hs6st*) genes during tracheal development.

Correspondence to Hiroshi Nakato: nakat003@umn.edu

Abbreviations used in this paper: *bnl, branchless*; *btl, breathless*; HS, heparan sulfate; HSPG, heparan sulfate proteoglycan; *Hs2st*, heparan sulfate 2-*O* sulfotransferase; *Hs6st*, heparan sulfate 6-*O* sulfotransferase; *sfl*; *sulfateless*; *trh, trachealess*.

The online version of this article contains supplemental material.

The Journal of Cell Biology, Vol. 174, No. 6, September 11, 2006 773–778
http://www.jcb.org/cgi/doi/10.1083/jcb.200603129

Results and discussion

We generated *Hs2st* and *Hs6st* mutations by imprecise P-element excision (Fig. S1, available at http://www.jcb.org/cgi/content/full/jcb.200603129/DC1). The excision alleles, $Hs2st^{d267}$ and $Hs6st^{d770}$, delete their respective coding regions, and lethality of $Hs2st^{d267}$ and $Hs6st^{d770}$ homozygotes was equivalent to that of their deficiency transheterozygotes, indicating that these mutants are null alleles for each gene. Despite the previous implication of 2-*O* and 6-*O* sulfate groups in the binding of HS to many growth factors in vitro (for reviews see Nakato and Kimata, 2002; Habuchi et al., 2004), *Hs2st* and *Hs6st* mutants showed only moderate effects on development. Zygotic *Hs2st* and *Hs6st* mutants survive to the adult stage without showing obvious morphological defects. We also generated embryos in which both maternal and zygotic *Hsst* gene activities are eliminated ("*Hsst* null embryos"). Although such null mutations caused partial lethality during development, significant fractions of these null mutants survive to the adult stage without visible phenotypes. This finding demonstrated that loss of either 2-*O* or 6-*O* sulfation does not completely disrupt normal development.

Because 2-*O* and 6-*O* sulfations are critical for FGF-HS binding in vitro (for reviews see Nakato and Kimata, 2002; Habuchi et al., 2004), we focused our efforts on the function of *Hs2st* and *Hs6st* in *btl*-mediated tracheal migration. The tracheal system develops from clusters of ectodermal cells that invaginate into the underlying mesoderm and form ten sacs on each side of the embryo. Each sac forms six primary branches by stereotypical cell migration. Some of these branches, such as the dorsal trunk, fuse with corresponding branches in neighboring segments to form a continuous tracheal network (Fig. 1 A). In *btl* or *sfl* mutants, the tracheal cells remain clustered at the site of the tracheal pits without migration (Klambt et al., 1992; Lin et al., 1999). In contrast, we found that maternal and zygotic null mutations of *Hs2st* or *Hs6st* had only limited effects on tracheal development (Fig. 1, D–F). Remarkably, only 9% of *Hs2st* null embryos exhibited a stalled migration of the dorsal branch (Fig. 1 D). A fraction (39%) of *Hs6st* null embryos exhibited tracheal defects (Fig. 1 E). In these mutant embryos tracheal migration is incomplete, as revealed by the presence of large gaps in the dorsal trunks, as well as stalled tracheal branches. The migration defects in these embryos were observed in all primary branches, but most commonly in the dorsal branch and the dorsal trunk. Surprisingly, however, tracheal morphology was indistinguishable from that of wild-type embryos in the remaining 61% of the embryos (Fig. 1 F).

Next, we examined whether *Hs2st* and *Hs6st* mutations affect the formation of the tracheoblast in the wing disc. Normal development of tracheoblasts was observed in all *Hs2st* and most *Hs6st* mutants we examined (Fig. 1, I and J), although the tracheoblast was slightly reduced in size in a small fraction (18%) of *Hs6st* mutant discs (Fig. 1, K and L). The small tracheoblast phenotype of *Hs6st* mutants was completely rescued by *Hs6st* expression from a *UAS-Hs6st* transgene (Fig. 1 M). Thus, null mutations in *Hs2st* and *Hs6st* do not completely block *btl*-mediated tracheal formation, showing that *Hs2st* and *Hs6st* mutant animals can produce HS chains that retain a considerable level of activity to mediate FGF signaling.

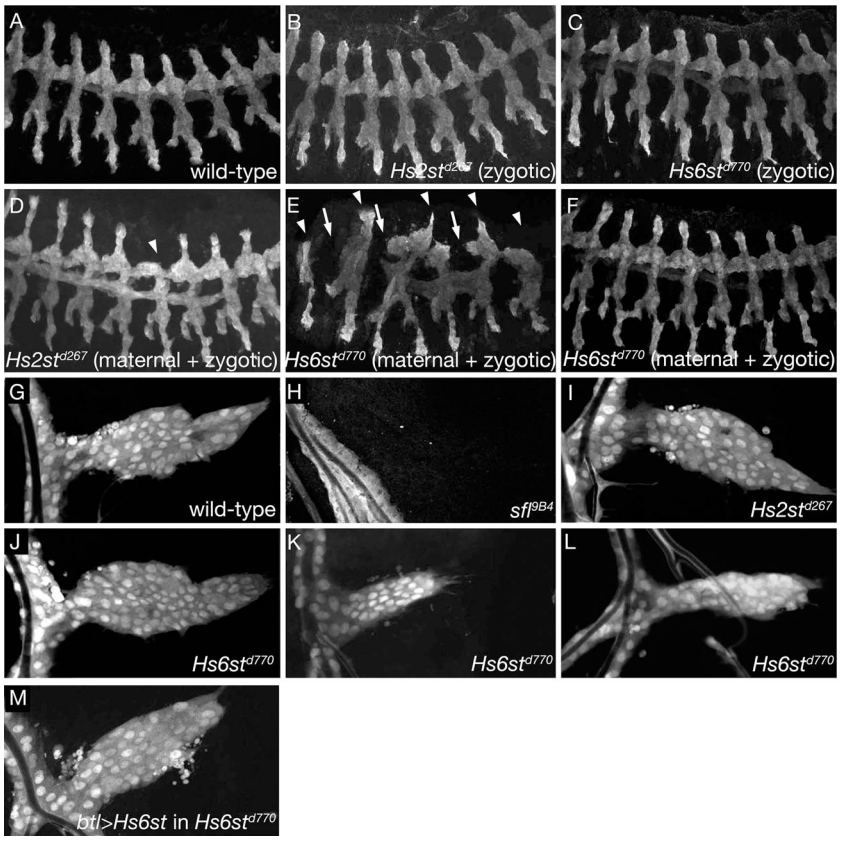

Figure 1. **Tracheal phenotypes of *Hs2st* and *Hs6st* mutants.** (A–F) Embryonic tracheal phenotypes in *Hs2st* and *Hs6st* mutants. Tracheal phenotypes were observed in stage 14 embryos using enhancer trap activity for the *trachealess* (*trh*) gene. (A) Wild-type embryos. $Hs2st^{d267}$ (B) or $Hs6st^{d770}$ (C) zygotic mutations do not affect tracheal development. (D) $Hs2st^{d267}$ maternal and zygotic null mutations have little effect on tracheal morphology except for migration defects of the dorsal branch (arrowhead) in 9% of these embryos. (E) 39% (20 out of 51) of $Hs6st^{d770}$ null embryos showed tracheal migration defects. Abnormalities were commonly observed in the dorsal trunk (arrows) and the dorsal branch (arrowheads). The other embryos (61%) showed normal tracheal morphology (F). (G–M) Tracheoblast formation in $Hs2st^{d267}$ and $Hs6st^{d770}$ wing discs. Tracheoblasts were visualized by *UAS-GFP* driven by *btl-Gal4* (G, I, J, K, L, and M) or *trh* enhancer trap expression (H). (G) Wild-type tracheoblasts. sfl^{9B4} mutation causes loss of tracheoblasts (H). Overall morphology of the tracheoblasts was not affected in all $Hs2st^{d267}$ (I) and most $Hs6st^{d770}$ (J) mutants. Two examples are shown for $Hs6st^{d770}$ mutant discs with smaller tracheoblasts (K and L). This phenotype was completely rescued by *Hs6st* expression in *btl-Gal4/UAS-Hs6st;* $Hs6st^{d770}$ (M).

The modest tracheal phenotypes of the *Hs2st* and *Hs6st* null mutants clearly challenge a current view on the role of HS fine structures: numerous biochemical analyses have demonstrated that 2-*O* and 6-*O* sulfate groups are critically required for the HS-growth factor interaction (for reviews see Nakato and Kimata, 2002; Habuchi et al., 2004). One possible reason for the restricted phenotypes of these mutants is that the sulfation patterns of mutant HS are altered to restore the growth factor signaling. To examine this possibility, disaccharide profiles of HS from *Hs2st* and *Hs6st* mutant animals were determined using fluorometric post-column HPLC (Toyoda et al., 2000). In wild-type adult flies, the disaccharide composition of HS showed a similar pattern to representative vertebrate tissues (Toyoda et al., 2000). In contrast, HS samples from *Hs2st* or *Hs6st* zygotic mutant adults showed a complete loss of the corresponding disaccharide units, confirming the amorphic nature of these mutant alleles. Significantly, HS disaccharides from *Hs2st* mutants showed not only a loss of 2-*O* sulfated disaccharide units, but also a remarkable increase of 6-*O* sulfated disaccharides. Similarly, levels of the 2-*O* sulfated disaccharides are strikingly elevated in *Hs6st* mutants. As a result, the level of total sulfate groups on HS was not affected in each case, and the total charge of HS in *Hs2st* and *Hs6st* mutants was almost wild type (Fig. 2). These results strongly suggested the existence of a compensation mechanism that adjusts the levels of sulfate groups when a component of the HS-modification machinery is lacking. Importantly, similar compensation of HS sulfation has also been observed in *Hs2st* mutant mice (Merry et al., 2001), implicating this system as a general property of the HS modification machinery that is widely conserved across species. Thus, the unaltered charge levels on HS in the *Drosophila Hsst* mutants may contribute to their mild phenotypes, and the function of the 2-*O* sulfate group seems to be replaceable with that of the 6-*O* sulfate group, and vice versa, in some developmental contexts.

To confirm the hypothesis that the compensatory increase of sulfation weakens *Hs2st* and *Hs6st* mutant phenotypes, we performed several sets of experiments in which the compensation was blocked. First, we examined the tracheal phenotypes of *Hs2st*; *Hs6st* double-mutant animals. In these animals, the compensation of HS sulfation would not occur due to the absence of both counterparts (*Hs2st* and *Hs6st*) that complement each other in *Hs2st* or *Hs6st* single mutants. In fact, despite the relatively normal development of the single mutants, the *Hs2st; Hs6st* zygotic double mutants are completely lethal. In wild-type embryos, tracheal precursor cells invaginate in each hemisegment at stage 11 (Fig. 3 A), and migrate and elongate to form primary branches at stage 12 (Fig. 3 D). One of these branches, the dorsal trunk, fuses with ones in the neighboring segments at stage 14 (Fig. 3 G). Although invagination seems to occur normally in the *Hs2st; Hs6st* embryos, they exhibit several characteristic defects in branching morphogenesis. First, mutant tracheal precursor cells failed to migrate to form the primary branches (Fig. 3 H). This defect resembles that of *btl* or *sfl* mutants (Klambt et al., 1992; Lin et al., 1999). Second, clusters of mutant tracheal cells tend to extend dorsally and ventrally, forming long, skinny sacs of tracheal precursor cells of various size (Fig. 3, E and H). Finally, 16% of mutant embryos showed fusion of the tracheal sacs to those in the neighboring segments (Fig. 3, C and I).

We asked whether FGF signaling is impaired in these animals using an antibody that specifically recognizes the diphosphorylated form of MAP kinase (dpMAPK; Gabay et al., 1997). In wild-type embryos, dpMAPK is detected in the tracheal placodes at stage 10, reflecting activation of DER, a *Drosophila* EGF receptor (Gabay et al., 1997). This dpMAPK signal was not diminished in the *Hs2st; Hs6st* embryos, showing that *DER* signaling is not affected by the double mutations (Fig. 3, K, K'; Fig. S2 A, available at http://www.jcb.org/cgi/content/full/jcb.200603129/DC1). At stage 12, wild-type embryos show a strong dpMAPK signal in the migrating tip cells of each primary branch due to activation of FGF signaling (Gabay et al., 1997). In contrast, the *btl*-dependent MAPK activation in the tip cells is disrupted in the *Hs2st; Hs6st* embryos (Fig. 3, M, M'; Fig. S2 A). In situ RNA hybridization experiments revealed that *bnl* expression is not altered in the double mutant embryos (Fig. S2 C), confirming that the branching defects observed in the

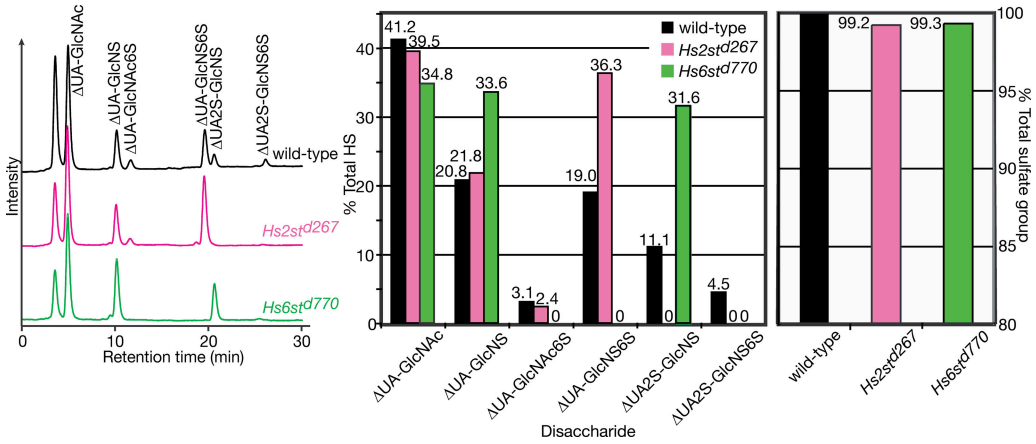

Figure 2. **HS disaccharide profiling of *Hs2st* and *Hs6st* mutants.** (Left) Representative HPLC chromatograms of wild-type (black), *Hs2st*^{d267} (pink), and *Hs6st*^{d770} (green) mutant HS. (Middle) Graphical depiction of disaccharide composition in these mutants, represented as percentage of total HS. (Right) Total levels of sulfate groups in *Hs2st*^{d267} and *Hs6st*^{d770} mutants. The value indicates the ratio of total sulfate groups in mutants to that in wild type.

double mutants are caused by disruption of FGF reception but not FGF expression. These results showed that HS with neither 2-*O* nor 6-*O* sulfate groups lost the ability to mediate Btl signaling.

Next, we examined whether simultaneous loss of both 2-*O* and 6-*O* sulfate groups affects tracheoblast formation in the wing disc. Because *Hs2st; Hs6st* mutants die during embryogenesis, we analyzed *Hs2st* homozygous animals bearing a transgene that expresses double-stranded RNA for *Hs6st* (*Hs6st* RNAi) under a specific Gal4 driver (Kennerdell and Carthew, 2000). Tracheoblast development was not affected either by homozygosity of the *Hs2st* null mutation (Fig. 1 I) or by expression of the *Hs6st* RNAi construct (unpublished data). In contrast, *Hs6st* RNAi in *btl*-expressing (tracheal) cells in *Hs2st* homozygous mutant background completely blocked the formation of the tracheoblast (Fig. 3 O). No such effect was observed, however, when the *Hs6st* RNAi was induced in *bnl*-expressing (nontracheal) cells in the same mutant background (Fig. 3 P). Thus, HS requires either 2-*O* or 6-*O* sulfate groups for reception of FGF, but these modifications are not essential in the FGF-expressing cells. Collectively, tracheal development could occur in *Hs2st* or *Hs6st* single mutants, but not in the double mutants. These findings demonstrated redundant roles of 2-*O* and 6-*O* sulfate groups of HS in FGF signaling during tracheal development.

As another approach to reduce 6-*O* sulfation without inducing an increase of other sulfation events, we examined the effects of overexpressing *Sulf1*, a *Drosophila* extracellular sulfatase (CG6725), on FGF signaling. Vertebrate *Sulf* genes encode secreted HS 6-*O* sulfatases, which remove sulfate groups from the HS on the cell surface (Dhoot et al., 2001). Because Sulf1 seems to modify HS fine structure extracellularly, and we hypothesized that compensatory changes in sulfation occur during HS biosynthesis in the Golgi, we expected that the number of sulfate groups on HS in *Sulf1*-expressing animals would decrease. Indeed, this was the case. Disaccharide profiling of HS from *actin-Sulf1* animals showed a significant reduction in the level of 6-*O* sulfation without the compensatory increase of other sulfate groups (Fig. 4 A). As a result, the total sulfate level is reduced in these animals to 76.3% of the wild-type level. Importantly, overexpression of *Sulf1* had stronger effects on viability and FGF-mediated tracheogenesis than *Hs6st* mutations. *actin-Sulf1* animals showed 71% lethality (unpublished data). The tracheoblast was dramatically reduced in size by expression of *Sulf1* in *btl*-expressing (tracheal) cells (Fig. 4 B). The fact that *Sulf1*-expressing animals show more severe phenotypes than *Hs6st* null mutants strongly suggests that the compensatory increase of 2-*O* sulfation in *Hs6st* mutant HS restores the ability to mediate FGF signaling. From these findings, we conclude that biosynthesis and modification of HS show a striking flexibility. In the absence of a component of the HS-modification machinery, living cells can form HS that lacks normal fine structures but retains normal levels of sulfate groups and a considerable level of activity for growth factor signaling.

Numerous in vitro studies have identified various ligand proteins that bind to specific sulfated HS sequences.

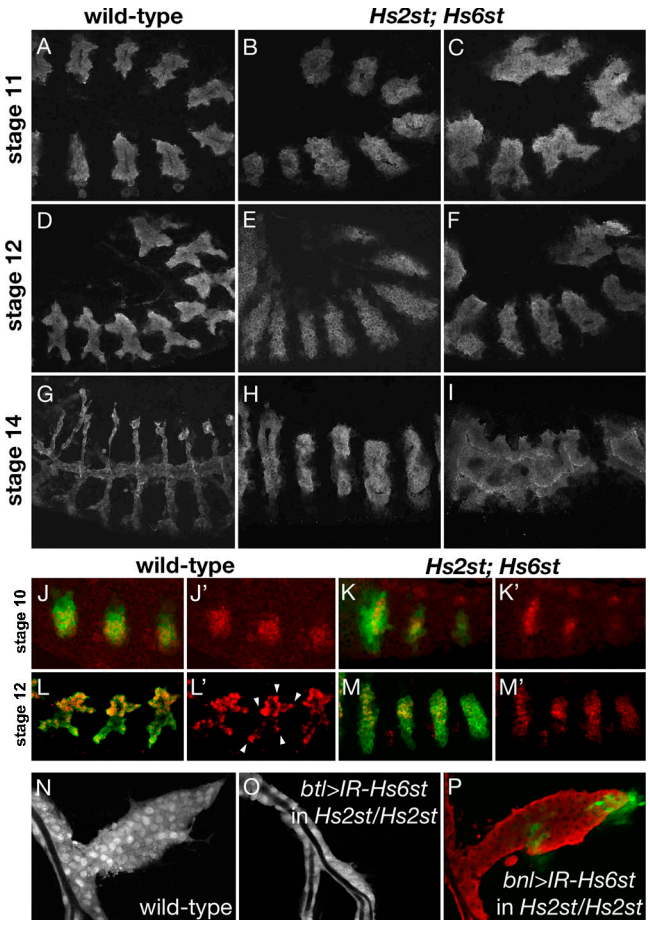

Figure 3. **Tracheal phenotypes and FGF-dependent MAPK activation in *Hs2st; Hs6st* double mutants.** (A–I) Embryonic tracheal phenotypes in *Hs2st; Hs6st* zygotic double mutants. Note that these *Hs2st; Hs6st* double mutants received some maternal contribution of both gene products. Embryonic tracheae were observed at stage 11 (A–C), 12 (D–F), and 14 (G–I) using *trh* enhancer trap. (A, D, and G) Wild-type embryos. (B, C, E, F, H, and I) Zygotic $Hs2st^{d267}$; $Hs6st^{d770}$ double mutants. (J–M) MAPK activation in wild-type and *Hs2st; Hs6st* double mutants. Tracheal cells and MAPK activation were marked by *trh* enhancer trap (green) and anti–diphospho-MAPK antibody (red), respectively, in wild-type (J and L) and the double mutant (K and M) embryos at stage 10 (J and K) and 12 (L and M). (N–P) Tracheoblast phenotypes in *Hs2st* wing discs expressing *Hs6st* RNAi. Tracheoblasts in wing discs were labeled by expression of *UAS-GFP* driven by *btl-Gal4* (N and O) or by *trh* enhancer trap (P). (N) Wild-type wing disc. (O) $Hs2st^{d267}$ *UAS-GFP/*$Hs2st^{d267}$*; btl-Gal4/ UAS-IR-Hs6st* wing disc. (P) Tracheoblasts (red) in $Hs2st^{d267}$ *UAS-GFP/* $Hs2st^{d267}$*; bnl-Gal4 1-eve-1/UAS-IR-Hs6st* wing disc. Expression of *bnl-Gal4* is shown by GFP (green).

Recent studies using animal models have also highlighted the importance of distinct HS sulfation patterns for HSPG functions (Bulow and Hobert, 2004). Thus, it is widely accepted that a specific sequence of sulfation on HS determines a binding site for a ligand, enabling HSPGs to interact selectively with proteins. However, it is not known how strictly ligand binding sites are defined in vivo. Our study demonstrated that living cells show an unexpected level of flexibility in biosynthesis and function of HS. In vivo HS sulfation is flexible in two ways. First, HS modifications can be adjusted in response to a defect in one type of sulfation. Second, mutant HS chains thus synthesized, which do not contain normal sequences of sulfate groups but

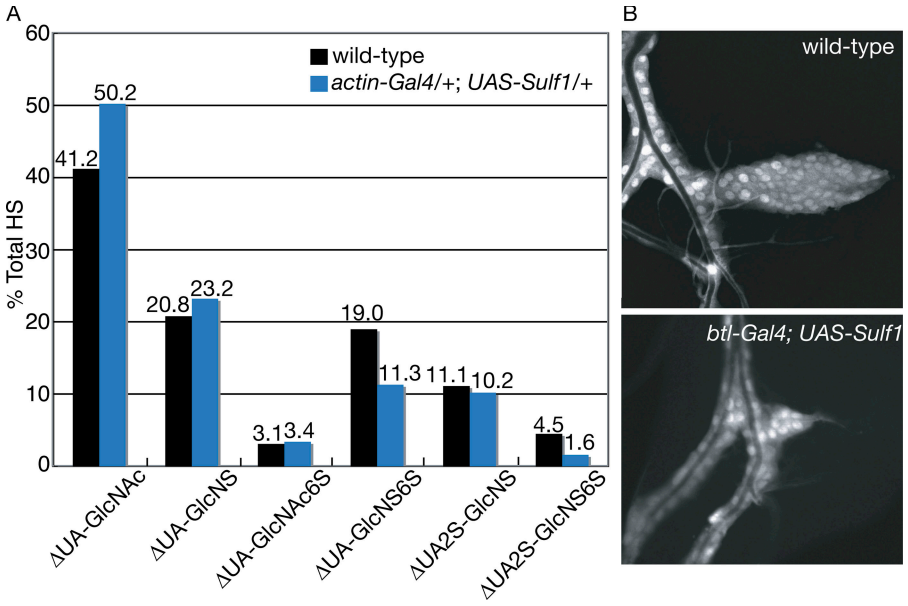

Figure 4. **Overexpression of *Sulf1* reduces the 6-*O* sulfate groups on HS and causes tracheal defects.** (A) HS disaccharide profiling of wild-type (black) and *actin-Gal4/+; UAS-Sulf1/+* (blue) animals. (B) Tracheoblast phenotypes in wild-type and *btl-Gal4 UAS-GFP/btl-Gal4; UAS-Sulf1* wing discs.

bear normal levels of sulfation, do not completely lose coreceptor activity for growth factor signaling.

We found that *Drosophila Hsst* mutations induce compensatory increases in sulfation at other positions, restoring a wild-type net charge on HS. Previously, Merry et al. (2001) showed that HS purified from $Hs2st^{-/-}$ embryonic fibroblasts did not have 2-*O* sulfate groups, but this loss was compensated for by increased *N*- and 6-*O* sulfation. This study suggested that a novel structure of HS found in the mutant HS may rescue some phenotypes of the $Hs2st^{-/-}$ mice. Our study provides evidence that the HS compensation indeed contributes to the modest phenotypes of animals deficient for these HS-modifying enzymes. The ability of the mutant HS to mediate signals is achieved, at least partly, by the sulfation compensation system because HS loses this ability when the compensation is blocked. These observations suggest that some in vivo roles of HS require a sufficient amount of sulfate groups but not a strictly defined placement on HS. This idea is supported by a recent biochemical study showing that binding of FGF to HS is dictated primarily by charge density rather than by the precise positioning of various sulfate groups (Kreuger et al., 2005; Jastrebova et al., 2006).

On the other hand, in different biological processes, specific sequences play essential roles in generating specificity of HS–protein interaction. In particular, sulfation at the 3-*O* position of the glucosamine residue, the rarest component of HS sulfation, is critically required for the binding site for antithrombin III (HajMohammadi et al., 2003) and a coat glycoprotein of herpes simplex virus (Shukla et al., 1999). Collectively, the mechanism for in vivo HS–protein interactions may occur by several mechanisms: (1) some proteins bind specific fine structures; (2) some proteins are attracted to the charge on HS but have less strict structural requirements; and (3) some proteins bind to HS based on a combination of specific sequence and charge density. Further studies will define ligand proteins in each class as well as the nature of their binding to HS.

Materials and methods

Fly stocks

The detailed information for fly strains used is described in Flybase (http://flybase.bio.indiana.edu/), except where noted. All flies were maintained at 25°C. The following strains were used: Oregon-R, wild-type strain; *P{GSV6}9303* (see the *Drosophila* Gene Search Project web site: http://218.44.182.94/%7Edclust/) and *P{lArB}A201.1M3*, P-element insertion lines for *Hs2st* and *Hs6st*, respectively; $Hs2st^{d267}$ and $Hs6st^{d770}$, null mutants for *Hs2st* and *Hs6st*, respectively (see below for mutant isolation); sfl^{9B4}, a null allele of *sfl*; *Df(2L)E55* (breakpoints, 37D02-E01; 37F05-38A01) and $Df(3R)ora^{l9}$ (breakpoints, 92B02-03; 92C02-03), chromosomal deficiency lines; *1-eve-1*, an enhancer trap line for the *trachealess* (*trh*) gene. The transgenic animals used were as follows: *UAS-GFPnls*; *UAS-FLP*; *UAS-Sulf1* (*Sulf1* cDNA (SD04414, Berkeley *Drosophila* Genome Project) was fused to a 344-bp *Sulf1* genomic PCR fragment to complete the coding region and inserted into pUAST vector); *UAS-IR-Hs6st* (see below for construction of *Hs6st* transgenic RNAi flies); *nanos-Gal4*; *actin-Gal4*; *btl-Gal4*; and *bnl-Gal4* (strain number 2211; *Drosophila* Genetic Resource Center, Kyoto Institute of Technology, Japan).

Isolation of *Hs2st* and *Hs6st* mutants

To generate $Hs2st^{d267}$ and $Hs6st^{d770}$ mutants, *P{GSV6}9303* and *P{lArB}A201.1M3* were exposed to P element transposase from $P\{ry^{+}, \Delta 2\text{-}3\}(99B)$. Their progeny were screened for loss of marker gene expression. Excision chromosomes were analyzed by PCR using flanking primers to find deletions, and the extent of each deletion was determined by sequencing PCR products that spanned the junction (see the legend to Fig. S1 for details). Lethality of $Hs2st^{d267}$ and $Hs6st^{d770}$ homozygotes (3.8% and 43%, respectively) was equivalent to that of their deficiency transheterozygotes ($Df(2L)E55/Hs2st^{d267}$ and $Df(3R)ora^{l9}/Hs6st^{d770}$, respectively), indicating that these mutants are null alleles for each gene.

Generation of embryos lacking maternal and zygotic function of *Hs2st* and *Hs6st*

Embryos lacking maternal and zygotic activity of *Hs2st* were obtained by crossing $Hs2st^{d267}$ homozygous females to $Hs2st^{d267}/CyO$ *wg-lacZ* males. To obtain *Hs6st* maternal and zygotic mutant embryos, germ line clones were generated using the autosomal FLP-DFS technique (Chou et al., 1993). Females carrying *nanos-Gal4 UAS-FLP/+; FRT82B* $Hs6st^{d770}/FRT82B$ ovo^{D1} were mated with $Hs6st^{d770}/TM3$ *Sb ftz-lacZ*. The resultant maternal and zygotic mutant embryos were identified with marked balancer.

Construction of *Hs6st* transgenic RNAi flies

Transgenic RNAi flies of *Hs6st* were obtained as described previously (Kamimura et al., 2004). A 500-bp-long cDNA fragment from the first

methionine was amplified by PCR and inserted as an inverted repeat (IR) into a modified pBluescript vector, pSC1, which possesses an IR formation site. IR-containing fragments were subcloned into pUAST, a transformation vector, and transformation of *Drosophila* embryos was performed using w^{1118} as a recipient strain.

Immunostaining and in situ RNA hybridization

Antibody staining was performed as described previously (Kamimura et al., 2004) using rabbit anti–β-galactosidase (1:500; Cappel) and mouse anti-diphosphorylated MAP kinase (1:200; Sigma-Aldrich). The primary antibodies were detected with Alexa Fluor–conjugated secondary antibodies (1:500; Molecular Probes). For quantitative analysis of MAPK activation, the percentage of segments that show normal dpMAPK staining in tracheal precursor cells (stage 10 wild type, $n = 12$; stage 10 *Hs2st; Hs6st*, $n = 18$; stage 12 wild type, $n = 27$; and stage 12 *Hs2st; Hs6st*, $n = 21$) was calculated. In situ RNA hybridization was performed as described previously (Kamimura et al., 2004). Light microscopy images were taken using a microscope (model BX50; Olympus) with a 40×/0.75 UPlanFl objective by a CCD camera (DP-50; Olympus) controlled by Studio Lite software. Confocal imaging was performed using a microscope (Axiovert 200M; Carl Zeiss MicroImaging, Inc.) with a 40×/0.75 Plan-Neofluar objective equipped with a confocal microscope system and a software (LCM5 PASCAL; Carl Zeiss MicroImaging, Inc.). Images were processed using Photoshop 7.0 (Adobe).

Preparation and HPLC analysis of HS disaccharides

HS disaccharide was analyzed by fluorometric post-column HPLC as described previously (Toyoda et al., 2000). Approximately 50 mg of lyophilized adult flies was used to isolate HS. The HS sample was digested with a heparitinase mixture (Seikagaku) and subjected to a reversed-phase ion-pair chromatography.

Online supplemental material

Fig. S1 shows the molecular characterization of *Hs2st* and *Hs6st* mutants. Fig. S2 shows the quantitative analysis of MAPK activation and in situ RNA hybridization of *bnl* mRNA in wild-type and $Hs2st^{d267}$; $Hs6st^{d770}$ embryos. Online supplemental material is available at http://www.jcb.org/cgi/content/full/jcb.200603129/DC1.

We are grateful to M. Sato, T. Aigaki, M. Krasnow, W.J. Gehring, W.L. Pak, the Developmental Studies Hybridoma Bank, the Bloomington Stock Center, Berkeley *Drosophila* Genome Project, and *Drosophila* Genetic Resource Center in Kyoto Institute of Technology for fly stocks and reagents. We also thank C. Kirkpatrick and A. Swearingen for critical reading of the manuscript and helpful comments.

This work was supported in part by the National Institutes of Health.

Submitted: 24 March 2006
Accepted: 7 August 2006

References

Bulow, H.E., and O. Hobert. 2004. Differential sulfations and epimerization define heparan sulfate specificity in nervous system development. *Neuron.* 41:723–736.

Chou, T.B., E. Noll, and N. Perrimon. 1993. Autosomal P[ovoD1] dominant female-sterile insertions in *Drosophila* and their use in generating germline chimeras. *Development.* 119:1359–1369.

Dhoot, G.K., M.K. Gustafsson, X. Ai, W. Sun, D.M. Standiford, and C.P. Emerson Jr. 2001. Regulation of Wnt signaling and embryo patterning by an extracellular sulfatase. *Science.* 293:1663–1666.

Gabay, L., R. Seger, and B.Z. Shilo. 1997. MAP kinase in situ activation atlas during *Drosophila* embryogenesis. *Development.* 124:3535–3541.

Habuchi, H., O. Habuchi, and K. Kimata. 2004. Sulfation pattern in glycosaminoglycan: does it have a code? *Glycoconj. J.* 21:47–52.

HajMohammadi, S., K. Enjyoji, M. Princivalle, P. Christi, M. Lech, D. Beeler, H. Rayburn, J.J. Schwartz, S. Barzegar, A.I. de Agostini, et al. 2003. Normal levels of anticoagulant heparan sulfate are not essential for normal hemostasis. *J. Clin. Invest.* 111:989–999.

Jastrebova, N., M. Vanwildemeersch, A.C. Rapraeger, G. Gimenez-Gallego, U. Lindahl, and D. Spillmann. 2006. Heparan sulfate-related oligosaccharides in ternary complex formation with fibroblast growth factors 1 and 2 and their receptors. *J. Biol. Chem.* 10.1074/jbc.M600806200.

Kamimura, K., J.M. Rhodes, R. Ueda, M. McNeely, D. Shukla, K. Kimata, P.G. Spear, N.W. Shworak, and H. Nakato. 2004. Regulation of Notch signaling by *Drosophila* heparan sulfate 3-O sulfotransferase. *J. Cell Biol.* 166:1069–1079.

Kennerdell, J.R., and R.W. Carthew. 2000. Heritable gene silencing in *Drosophila* using double-stranded RNA. *Nat. Biotechnol.* 18:896–898.

Klambt, C., L. Glazer, and B.Z. Shilo. 1992. *breathless*, a *Drosophila* FGF receptor homolog, is essential for migration of tracheal and specific midline glial cells. *Genes Dev.* 6:1668–1678.

Kreuger, J., P. Jemth, E. Sanders-Lindberg, L. Eliahu, D. Ron, C. Basilico, M. Salmivirta, and U. Lindahl. 2005. Fibroblast growth factors share binding sites in heparan sulphate. *Biochem. J.* 389:145–150.

Lin, X., E.M. Buff, N. Perrimon, and A.M. Michelson. 1999. Heparan sulfate proteoglycans are essential for FGF receptor signaling during *Drosophila* embryonic development. *Development.* 126:3715–3723.

Merry, C.L., S.L. Bullock, D.C. Swan, A.C. Backen, M. Lyon, R.S. Beddington, V.A. Wilson, and J.T. Gallagher. 2001. The molecular phenotype of heparan sulfate in the $Hs2st^{-/-}$ mutant mouse. *J. Biol. Chem.* 276:35429–35434.

Nakato, H., and K. Kimata. 2002. Heparan sulfate fine structure and specificity of proteoglycan functions. *Biochim. Biophys. Acta.* 1573:312–318.

Sato, M., and T.B. Kornberg. 2002. FGF is an essential mitogen and chemoattractant for the air sacs of the *Drosophila* tracheal system. *Dev. Cell.* 3:195–207.

Schlessinger, J., A.N. Plotnikov, O.A. Ibrahimi, A.V. Eliseenkova, B.K. Yeh, A. Yayon, R.J. Linhardt, and M. Mohammadi. 2000. Crystal structure of a ternary FGF-FGFR-heparin complex reveals a dual role for heparin in FGFR binding and dimerization. *Mol. Cell.* 6:743–750.

Shukla, D., J. Liu, P. Blaiklock, N.W. Shworak, X. Bai, J.D. Esko, G.H. Cohen, R.J. Eisenberg, R.D. Rosenberg, and P.G. Spear. 1999. A novel role for 3-*O*-sulfated heparan sulfate in herpes simplex virus 1 entry. *Cell.* 99:13–22.

Sutherland, D., C. Samakovlis, and M.A. Krasnow. 1996. *branchless* encodes a *Drosophila* FGF homolog that controls tracheal cell migration and the pattern of branching. *Cell.* 87:1091–1101.

Toyoda, H., A. Kinoshita-Toyoda, B. Fox, and S.B. Selleck. 2000. Structural analysis of glycosaminoglycans in animals bearing mutations in *sugarless, sulfateless*, and *tout-velu. Drosophila* homologues of vertebrate genes encoding glycosaminoglycan biosynthetic enzymes. *J. Biol. Chem.* 275:21856–21861.